

A “poor man’s approach” to modelling of micro-structured optical fibres

Jesper Riishede

Research Center COM, Technical University of Denmark, DK-2800 Kgs. Lyngby, Denmark

Niels Asger Mortensen

Crystal Fibre A/S, Blokken 84, DK-3460 Birkerød, Denmark

Jesper Lægsgaard

Research Center COM, Technical University of Denmark, DK-2800 Kgs. Lyngby, Denmark

Abstract. Based on the scalar Helmholtz equation and the finite-difference approximation, we formulate a matrix eigenvalue problem for the calculation of propagation constants, $\beta(\omega)$, in micro-structured optical fibres. The method is applied to index-guiding fibres as well as air-core photonic bandgap fibres, and in both cases qualitatively correct results are found. The strength of this approach lies in its very simple numerical implementation and its ability to find eigenmodes at a specific eigenvalue, which is of great interest, when modelling defect modes in photonic bandgap fibres.

Submitted to: *J. Opt. A: Pure Appl. Opt.*

1. Introduction

Since the first results on photonic crystal fibres [1] (PCF) many exciting phenomena have been reported (for a recent review see *e.g.* Ref. [2] and references therein). From the very start, a great emphasis has been on the modelling of the optical properties and frameworks of high complexity have been developed. In this work, we develop a “poor man’s approach” which allows for easy implementation and calculation of the propagation constant, $\beta(\omega)$, in arbitrarily microstructured fibres. Most approaches start from the fundamental vectorial wave equation for an isotropic dielectric medium

$$\nabla \times \frac{1}{\varepsilon(\mathbf{r})} \nabla \times \mathbf{H}(\mathbf{r}) = k^2 \mathbf{H}(\mathbf{r}) \quad (1)$$

where $k = \omega/c$ and $\varepsilon(\mathbf{r})$ is the dielectric function, which may be frequency dependent. For a fibre geometry with $\varepsilon(\mathbf{r}) = \varepsilon(x, y)$, *i.e.*, translational invariance along the z -direction, we look for solutions of the form $\mathbf{H}(\mathbf{r}) = \mathbf{h}(x, y)e^{i\beta z}$. Substituting this ansatz into the wave equation results in an eigenvalue problem, which determines

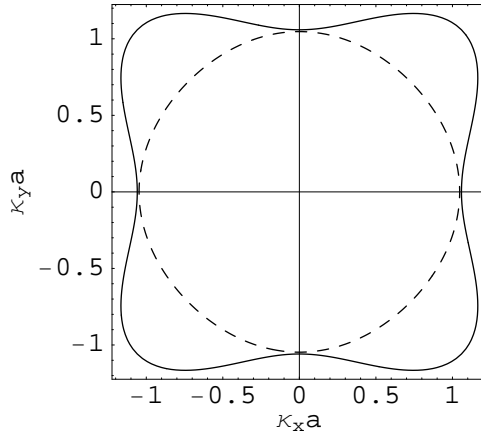


Figure 1. Contour plot of Eq. (6) for $\omega^2 = \frac{c^2}{\varepsilon} [\beta^2 + K^2]$ shown by the dashed line. For the region enclosed by the solid line, the relative error of the finite-difference approximation is generally less than 9%, and the relative error is zero at the origo ($\kappa_x = \kappa_y = 0$) where $\omega^2 = \frac{c^2}{\varepsilon} \beta^2$.

the dispersion $\omega(\beta)$. In the literature, it is often emphasized that in general a fully-vectorial approach is required for quantitative modelling of micro-structured fibres. Several fully-vectorial approaches have been reported including plane-wave methods [3, 4], multi-pole methods [5, 6], localised-function methods [7, 8], and finite-element methods [9]. The complicated implementation is common to all these methods. In this work, we present a “poor man’s approach” for calculating the propagation constant, $\beta(\omega)$, in arbitrary dielectric structures. Despite its obvious shortcomings, we believe it is far more useful for more qualitative studies as well as for teaching of the physics of micro-structured optical fibres at the introductory level.

2. Theory

2.1. The scalar Helmholtz wave-equation

We start from the scalar Helmholtz wave-equation

$$\left(\frac{\partial^2}{\partial x^2} + \frac{\partial^2}{\partial y^2} + \varepsilon(x, y)k^2 \right) \Psi(x, y) = \beta^2 \Psi(x, y) \quad (2)$$

with Ψ being the scalar field. In this approximation, we have neglected a logarithmic derivative of the dielectric function at the interfaces between *e.g.* SiO_2 and air. We also note that polarisation effects and/or degeneracies may only be fully revealed by a fully-vectorial approach. The strength of the scalar approach is that it is straight forward to implement and thus serves as an excellent starting point for researchers and students entering the field of micro-structured optical fibres. Furthermore, the Helmholtz equation (2) allows for an easy incorporation of effects like material dispersion, $\varepsilon(\omega)$.

2.2. The finite-difference approximation

Equation (2) constitutes an eigenvalue problem from which $\beta(\omega)$ can be calculated. We take the probably most simple approach based on a finite difference approximation of the Laplacian. For a quadratic grid with j labeling the grid points with spacing a we *e.g.* get the symmetrized representation of the Laplacian

$$\frac{\partial^2}{\partial x^2} f[x = ja] \approx \frac{1}{a^2} (f[(j+1)a] + f[(j-1)a] - 2f[ja]) \quad (3)$$

corresponding to nearest-neighbour coupling of the grid points. We can thus rewrite Eq. (2) as a matrix eigenvalue problem

$$\Theta \Psi = \beta^2 \Psi \quad (4)$$

with

$$\Theta_{ji} = \begin{cases} -4K^2 + \varepsilon_j k^2 & j = i \\ K^2 & j, i \text{ nearest neighbours} \\ 0 & \text{otherwise} \end{cases} \quad (5)$$

where $K = 1/a$. For the dielectric function we have $\varepsilon_j = \varepsilon(x_j, y_j)$ where (x_j, y_j) is the coordinates of the j th lattice point. The numerical task thus consists of finding eigenvalues of the matrix Θ , which is easily done using standard numerical libraries. The matrix is highly sparse, symmetric and when the dielectric function is real, it is even Hermitian. The numerical accuracy of the approximation is of course increased by decreasing the lattice constant.

2.3. The homogeneous case

In order to estimate the required size of a , we first consider the homogeneous case where $\varepsilon_j = \varepsilon$. This problem is well-known from solid state theory; it can be diagonalized by a plane wave ansatz, which results in the usual cosine-band result

$$\omega^2 = \frac{c^2}{\varepsilon} [\beta^2 + 2K^2(2 - \cos \kappa_x a - \cos \kappa_y a)]. \quad (6)$$

This result also has the correct asymptotic behaviour of the homogeneous-space solution

$$\omega^2 \simeq \frac{c^2}{\varepsilon} [\beta^2 + \kappa_x^2 + \kappa_y^2] + \mathcal{O}(a^2) \quad (7)$$

and by choosing a sufficiently small, the numerical discretisation is a good approximation to the solution of the exact problem. Because of the discretisation procedure, Eq. (6) has a finite band-width of $\frac{c^2}{\varepsilon} \times 8K^2$, *i.e.*,

$$\begin{aligned} & \max\{2K^2(2 - \cos \kappa_x a - \cos \kappa_y a)\} \\ & - \min\{2K^2(2 - \cos \kappa_x a - \cos \kappa_y a)\} = 8K^2. \end{aligned} \quad (8)$$

This means that only frequencies satisfying

$$\frac{c^2}{\varepsilon} \beta^2 \leq \omega^2 \leq \frac{c^2}{\varepsilon} [\beta^2 + 8K^2] \quad (9)$$

can be accounted for by the discretisation procedure. In the low-frequency regime, the relative error of the finite-difference approximation becomes small, and typically we should be limiting ourselves to *e.g.*,

$$\omega^2 < \frac{c^2}{\varepsilon} [\beta^2 + K^2] \Leftrightarrow a < (\varepsilon \omega^2 / c^2 - \beta^2)^{-1/2} \quad (10)$$

where the relative error of the finite-difference approximation is less than 9%, see Fig. 1. For higher frequencies, the finite-difference procedure becomes an inaccurate approximation to the exact problem, because of artificial band-structure effects.

2.4. The boundary problem

In principle Θ is infinite and for the implementation we obviously need to truncate the matrix. This truncation may affect the accuracy of the calculation. However, we are also faced with the problem of deciding how the finite-difference representation of the differential operators (in our case the Laplacian) are represented on the boundary of the calculation domain. This problem arises because calculation of finite differences on the boundary requires the use of points that fall outside the calculation domain. Thus, we have to determine a proper way of how these non-existing points should be treated.

In the definition of the Θ -matrix, we have simply chosen to neglect the points that fall outside the calculation domain. This is done in order to limit the complexity of the Θ -matrix, and thereby keep the formulation of the problem as simple as possible. The consequence of this simplification is that we impose the condition that the field has to be zero on the boundaries of the calculation domain. Naturally, this assumption will have an effect on the accuracy of the calculation, but the better the field is confined within the calculation domain, the better the truncated problem resembles the correct solution, since a zero amplitude on the boundary becomes a reasonable approximation in this case.

3. Modelling of Photonic Crystal Fibres

3.1. Numerical Implementation

Once the theory of the finite difference approximation has been established, the task of finding solutions to the scalar wave equation may be viewed as two subproblems. First, the Θ -matrix has to be created from a given dielectric structure, and secondly the eigenvalues, β^2 , and the corresponding eigenvectors, Ψ , have to be found. We have chosen to make our implementation in *Matlab*, because it provides effective tools for solving both these problems.

To give a more precise description of our implementation, we consider an example where an arbitrary dielectric structure has been discretized in a 100×100 grid. In this case Θ becomes a matrix with 10000×10000 elements, which indicates that the finite difference approach is very demanding in terms of memory consumption. However, as most of the elements of Θ are zero, it is advantageous to store Θ as a sparse matrix, which is easily done with the *Sparse-type* in *Matlab*. For an $n \times n$ dielectric structure, we need to store n^4 elements in the full representation, while only $\sim 5n^2$ elements are required in the sparse representation. Obviously, this gives rise to a dramatic decrease in the memory consumption, and thereby a corresponding increase in the size of the dielectric structures that may be examined.

The second problem we are faced with, concerns the search for eigenvalues, β^2 , and their corresponding eigenvectors Ψ . In the sparse representation, a complete diagonalization of the Θ -matrix may be performed, but this straightforward method has the disadvantage of being numerically heavy (and thus time consuming) since it calculates all n^2 eigenvalues. Typically, we are only interested in solving for a

few eigenvalues, e.g the largest values of β^2 , and this is a common feature of several advanced eigensolver libraries. In our implementation we use the *EIGS* command in *Matlab* which is based on the ARPACK-library [11]. As a further advantage, the *EIGS* command has the option of finding eigenvalues around a specified value, which may be particularly useful once a region with guided modes has been found.

3.2. Index-guiding Fibres

As a first example, the finite-difference method is applied to an index-guiding micro-structured fibre. Figure 2a shows the square dielectric structure used in the calculation, which we have chosen to discretize in a 128×128 grid. The dielectric structure has a width of $3\sqrt{3}\Lambda$, where Λ is the hole spacing, and it consists of air holes with a diameter of 0.4Λ placed in a silica background ($n=1.45$). A single air hole has been omitted in the center of the structure to create a waveguide core. In the case of index-guiding fibres, the fundamental mode corresponds to the eigenvector with the largest eigenvalue. Figure 2a shows the field distribution of the fundamental mode calculated at a normalized wavelength of $\lambda/\Lambda = 0.15$, and it is seen to be well confined to the core region.

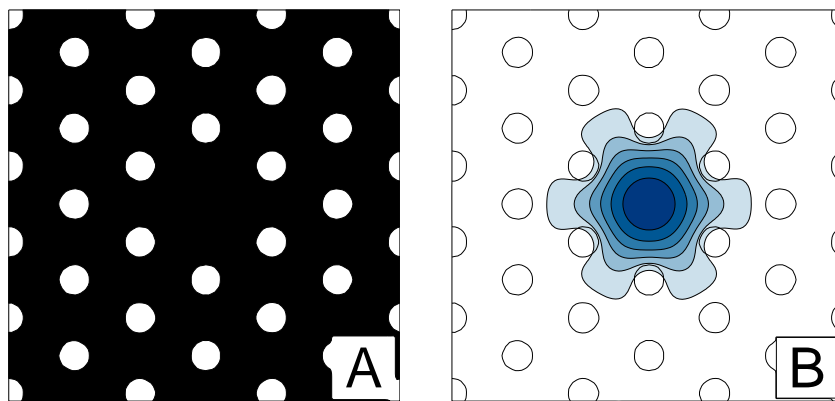


Figure 2. (A) A dielectric structure of an index-guiding photonic crystal fibre, with a normalized holediameter of $D/\Lambda = 0.4$. For the calculation the structure has been discretized in 128×128 points. (B) The field distribution of the fundamental mode, calculated at a normalized wavelength of $\lambda/\Lambda = 0.15$.

In figure 3 we have mapped out the effective mode index of the fundamental mode for several values of the normalized wavelength. For comparison, we have included a finite-difference calculation, where the width of the calculation domain has been increased to $6\sqrt{3}\Lambda$. Finally, we have included fully-vectorial results for a fully-periodic hole-structure, with a repeated defect, obtained in a plane-wave basis using periodic boundary conditions [4]. The dielectric structure used in this calculation consist of 6 simple cells, and is thus similar to the structure in figure 2a.

By comparing the finite-difference calculations for the small and the large calculation domain, we are able to see the effect of the truncation. For the small calculation domain, we find that the calculated value of the effective mode-index decreases rapidly for long normalized wavelengths. This is because the field distribution extends to the edge of the calculation domain, and thus the assumption of

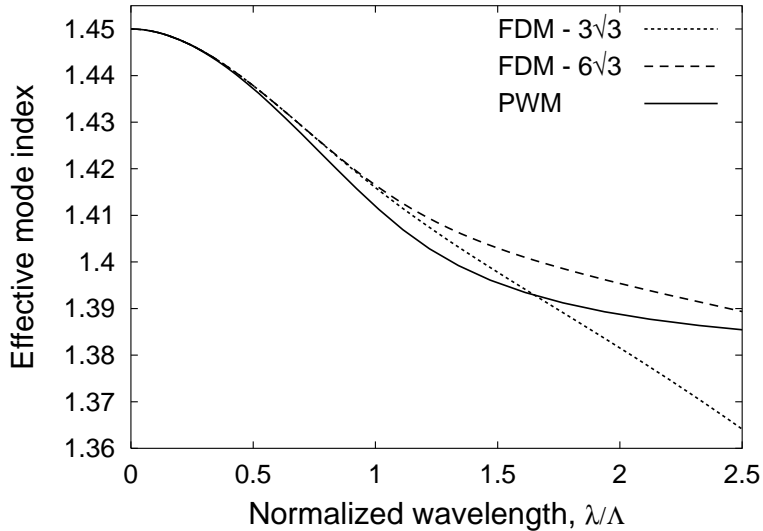


Figure 3. Comparison of the mode-index for the fundamental mode in an index-guiding PCF with a hole diameter of 0.4Λ . The dotted curves are calculated by the finite-difference method (FDM) for two different widths of the dielectric structure, while the solid curve is calculated by the plane-wave method (PWM).

a zero amplitude on the edge is no longer valid. Consequently, the field will penetrate into the air holes, and thereby cause a lowering of the effective mode index. By increasing the width of the calculation domain, we are able to shift the onset of this effect towards larger values of the normalized wavelength.

In the comparison between our scalar finite-difference approach and a full-vectorial method, we find that the scalar approach gives qualitative correct results and accounts well for the overall wavelength dependence. However, especially for the long wavelengths the simple approach becomes inaccurate because of the scalar approximation, and the scalar approach is seen to overestimate the value of the effective mode-index. For $\lambda \sim \Lambda$ the strong proximity of the air-holes require a correct treatment of the air-silica boundary conditions which can only be quantitatively accounted for by a fully-vectorial approach.

3.3. Photonic Bandgap-guiding Fibres

In the literature, it is often argued that accurate modelling of photonic bandgap materials requires the use of a full-vectorial method. This is true for all photonic crystals of practical interest, because it is required that they have a large index-contrast in order to obtain large bandgaps. However, this may lead to the incorrect conclusion that photonic bandgaps and defect modes are pure full-vectorial phenomena. From a theoretical point of view bandgaps do not arise as a consequence of coupling between field components at a dielectric interface, as it is the case in a full-vectorial method. Rather, they are a fundamental property of applying the wave equation to a periodic waveguide structure, and thus photonic bandgaps and defect modes can also exist in a scalar calculation.

The question is how well a scalar calculation actually approximates the results in photonic bandgap fibres, where the scalar wave equation is obviously not a correct representation of the actual physical problem. In order to examine this, we have chosen to apply our finite-difference method to the extreme case of airguiding photonic bandgap fibres. The dielectric structure used in our calculation is shown in figure 4a. It has a width of $6\sqrt{3}\Lambda$ and consists of an air-silica cladding structure with a hole diameter of $D = 0.88\Lambda$. The core defect is made by inserting a large air hole with a diameter of 2.65Λ . For the calculation, we discretized the structure in 256×256 grid points. We have chosen this specific structure, because it is known to support guided modes in a full-vectorial calculation [12].

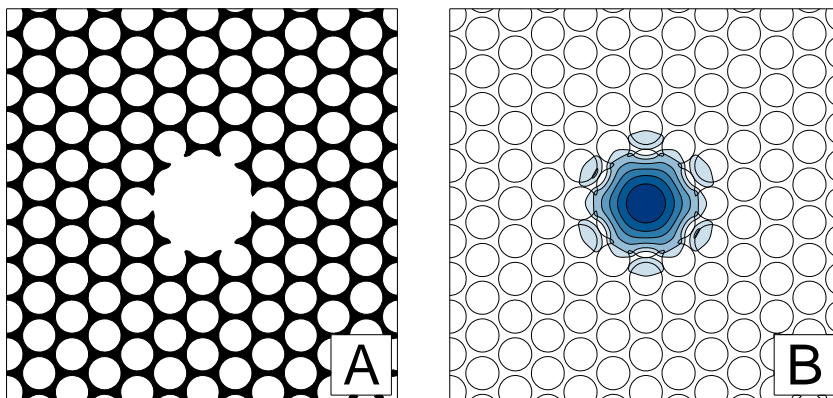


Figure 4. (A) The dielectric structure of an airguiding photonic bandgap fibre discretized in 256×256 points. The cladding structure has a hole diameter of 0.88Λ while the core defect is created by inserting a large air hole with a diameter of 2.65Λ . (B) The field distribution of the fundamental mode in the airguiding photonic bandgap fibre, calculated at a normalized wavelength of $\lambda/\Lambda = 0.7$.

A disadvantage of this finite-difference implementation is that there is no simple way of calculating the position of the photonic bandgaps. Therefore, we have used a full-vectorial planewave-method to calculate the bandgaps of an infinite triangular lattice with a hole diameter of 0.88Λ . Once the position of the photonic bandgaps have been located, it is possible to search for a defect mode. As already mentioned, the *EIGS*-command in *Matlab* has the useful ability to find eigenvectors around a specified eigenvalue. This is particularly useful for bandgap fibres, since the defect mode appears as an isolated eigenmode inside the boundaries of the photonic bandgap.

By choosing a normalized wavelength of $\lambda/\Lambda = 0.7$ and searching for an eigenvalue for which $\beta \approx k$, the scalar finite-difference method finds a defect mode localized to the core region. The field distribution of this defect mode is shown in figure 4b. For simplicity we have chosen to depict the absolute value of the field distribution. Therefore, the 6 lobes surrounding the central defect do in fact have the opposite amplitude of the field inside the defect. These 6 resonances are a common feature of airguiding fibres, and they are also found in a full-vectorial calculation.

In figure 5 we have mapped out the effective mode-index for a range of the normalized wavelength. For comparison we have included the guided modes and the bandgap edges from a full-vectorial calculation. Both methods are found to predict the existence of a fundamental and a second-order mode, and a reasonable agreement

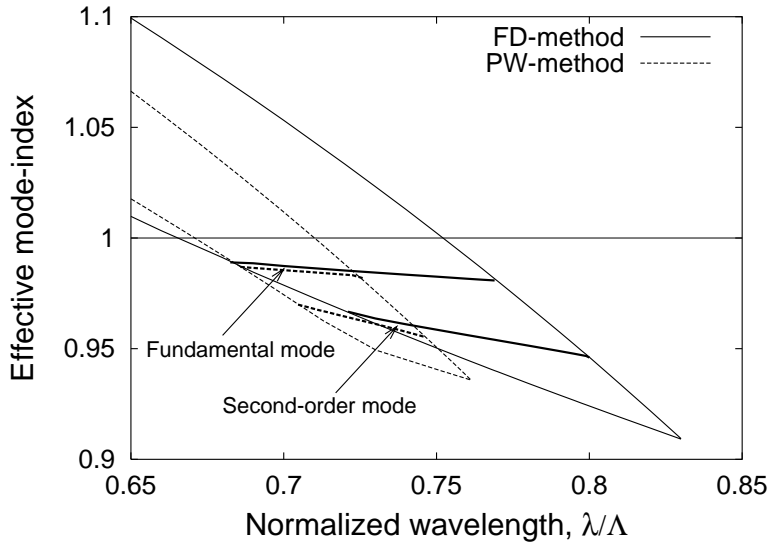


Figure 5. Comparison of the scalar finite-difference method (FD-method) and the full-vectorial planewave-method (PW-method) for an airguiding photonic bandgap fibre. A strong resemblance between the methods is found for both the fundamental and the second-order mode, but the finite-difference is seen predict reasonably wider bandgaps.

is found between the results of the two methods. However, we generally find that the finite-difference method overestimates the values of the effective mode-index.

The major difference between the full-vectorial and the scalar calculation is that the latter is seen to predict significantly increased bandgaps. This naturally gives rise to a much wider range in which the structure supports a confined mode. The bandedges in the scalar calculation have been found as the modes that lie just above and just below the defect modes. As the bandedge-modes are in fact cladding modes, and thus well distributed over the entire cross section of the dielectric structure, they are more affected by the truncation of the Θ -matrix than the well confined defect modes. We have tried to increase the width of the calculation domain and also the number of grid points, but this is not found to have any influence on the overall result. It is therefore believed that the increased bandgap size is a consequence of the scalar approximation.

The final result indicates, that although a scalar approach provides great insight to the basic physics of photonic bandgap fibres, it cannot reveal the complete picture. This is not really surprising. However, we still believe that this method is of great interest, mainly due to its simple implementation. Also, the model can easily be expanded to include periodic boundary conditions and a full-vectorial implementation is feasible as well.

4. Conclusion

The field of photonic crystal fibres has by now existed for almost a decade and the results of the research efforts will probably soon move inside the classroom and also

be found in text-book material on fibre optics and electro-magnetic theory of photonic crystals. This also calls for simple approaches to modelling of micro-structured optical fibres which are easy to implement and which without too much effort can produce results which are in qualitative agreement with those observed in real micro-structured fibres. We believe that the present work provides such a simple approach.

In order to limit the complexity of the mathematical formulation of the problem, we have considered a scalar wave-equation which is solved by means of the most simple numerical approach to differential equations; the finite-difference approximation. With appropriate boundary conditions this results in a matrix eigenvalue problem. The matrix, Θ , of this problem is highly sparse and has very simple analytical matrix elements which only depend on the lattice spacing, the frequency, and the dielectric function. Thus, no implementation of complicated basis functions is required. For a given frequency ω the propagation constant β can easily be found by finding the eigenvalues of Θ . By the aid of standard numerical routines, we are able to solve for a specific number of eigenvalues closest to a specified value. This is particularly useful for bandgap guiding fibres, where the modes of interest corresponds to either the smallest or the largest eigenvalue, but are placed in an interval determined by the photonic bandgap edges.

In conclusion we find that the presented finite-difference method, apart from being simple to implement and despite the extremely simple model, is able to provide qualitative correct results for both index-guiding and photonic bandgap guiding fibres. The latter case is quite surprising, since modelling of photonic bandgap effects is normally associated with full-vectorial methods. Furthermore, we find that the method is robust and it is relatively simple to incorporate periodic boundary conditions, or to expand the model to a full-vectorial method. This holds interesting prospects for a future development of this method.

Acknowledgements

We acknowledge useful discussions with M. D. Nielsen and B. T. Kuhlmeij. J. L. is financially supported by the Danish Technical Research Council (STVF).

References

- [1] Knight J C, Birks T A, Russell P S J and Atkin D M 1996 *Opt. Lett.* **21** 1547–1549
- [2] Russell P 2003 *Science* **299** 358–362
- [3] Ferrando A, Silvestre E, Miret J J, Andrés P and Andrés M V 1999 *Opt. Lett.* **24** 276–278
- [4] Johnson S G and Joannopoulos J D 2001 *Opt. Express* **8** 173–190
- [5] White T P, Kuhlmeij B T, McPhedran R C, Maystre D, Renversez G, de Sterke C M and Botton L C 2002 *J. Opt. Soc. Am. B* **19** 2322–2330
- [6] Kuhlmeij B T, White T P, Renversez G, Maystre D, Botton L C, de Sterke C M and McPhedran R C 2002 *J. Opt. Soc. Am. B* **19** 2331–2340
- [7] Mogilevtsev D, Birks T A and Russell P S J 1999 *J. Lightwave Technol.* **17** 2078–2081
- [8] Monro T M, Richardson D J, Broderick N G R and Bennett P J 2000 *J. Lightwave Technol.* **18** 50–56
- [9] Koshiha M and Saitoh K 2001 *IEEE Photon. Technol. Lett.* **13** 1313–1315
- [10] White T P, McPhedran R C, de Sterke C M, Botton L C and Steel M J 2001 *Opt. Lett.* **26** 1660–1662
- [11] ARPACK Numerical Library, <http://www.netlib.org/arpack>
- [12] Broeng J, Barkou S E, Søndergaard T and Bjarklev A 2000 *Opt. Lett.* **25** 96–98